Diphotons in a Nonlinear Fabry-Pérot Resonator: Bound States of Interacting Photons in an Optical "Quantum Wire"

Ivan H. Deutsch and Raymond Y. Chiao
Department of Physics, University of California, Berkeley, California 94720

John C. Garrison
Lawrence Livermore National Laboratory, University of California, Livermore, California 94550
(Received 8 September 1992)

We propose a high-Q Fabry-Pérot resonator with cylindrical mirrors, operating near fundamental mode and filled with an alkali vapor, as the photonic analog to the electronic quantum wire. The internal photons constitute a 1D Bose gas with pairwise interactions. We solve for the two-photon bound state which determines a resonance for the two-photon transmission function. Emphasis is placed on the experimental feasibility of observing these quasiparticles.

PACS numbers: 42.50.Dv, 05.30.Jp, 42.65.Jx

Lower-dimensional fermion systems have been intensively investigated in connection with electronic properties of solid-state materials, e.g., quantum dots, quantum wires, and quantum wells [1]. We extend the notion of dimensional reduction from fermionic to bosonic systems by proposing a realization of the optical quantum wire consisting of a high-Q cavity with cylindrical mirrors. The resonant cavity enhances the characteristic field strength of vacuum fluctuations, so that light in such a "quantum wire" filled with a nonlinear medium constitutes an experimentally realizable *interacting* 1D photon gas. When the interaction is attractive, photonic bound states can appear in the many-body system. We investigate the simplest case of the two-photon bound state, or "diphoton" [2].

We consider a Kerr medium in which classical evolution of a light wave is described by the nonlinear Schrödinger equation (NLSE). This equation has a rich variety of soliton solutions, but we will concentrate on self-trapping in one transverse dimension, in which linear diffraction is compensated by nonlinear self-focusing to yield a stable beam whose transverse intensity profile is constant with propagation [3]. In a traveling-wave configuration, these solitons have been observed in liquid carbon disulfide [4], glasses [5], and semiconductors [6], with promise for application to all-optical data processing.

Quantization of the 1D NLSE produces a theory of a nonrelativistic 1D Bose gas with pairwise interactions via delta-function potentials that can be either attractive or repulsive [7]. Exact energy eigenstates can be constructed using the Bethe Ansatz, of which the diphoton is the simplest example. One manifestation of this Bose gas is the quantum field theory associated with the optical fiber temporal soliton. Lai and Haus [8] and Wright [9] studied this problem in the large photon-number limit to examine corrections to the classical "bright" soliton by vacuum fluctuations. In this quasiclassical limit the vacuum fluctuations can become squeezed [10]. In the low photon-number limit Yurke and Potasek [11] analyzed the repulsive Bose gas associated with the "dark soliton," and predicted photon antibunching. However, because the nonlinearity is extremely small in silica fibers, experimental observation of interactive quantum effects in this regime is not feasible.

Experimental observation of the interacting Bose gas in the low photon-number limit requires an extremely large nonlinearity and strong spatial confinement of the photons. In a standing-wave geometry, the small bandwidth of the field allows near resonant excitation of an atomic vapor to produce a large nonlinearity, while simultaneously the field strength can be enhanced by confining the photons in a small volume of space. This dual resonant enhancement of the material response and of the field strength provides experimental access to the quantum field theory of nonlinear optics. By contrast, in a traveling-wave device such as an optical fiber or a planar waveguide (the configuration considered in our previous work [2]), enhancement of the field strength requires use of a broadband (short duration) pulse, which reduces the nonlinearity by dispersive effects. Thus optical waveguides are not good candidates for *interactive* quantum wires or wells since the photon-photon coupling is negligibly small.

The natural geometry we are led to is a high-Q Fabry-Pérot cavity with cylindrical mirrors, filled with an alkali vapor, e.g., cesium, and operating near the fundamental mode. This geometry locks out the dynamics in the longitudinal dimension (z), as well as one of the transverse dimensions (y), and leaves a continuum of modes in the remaining transverse dimension (x) (see Fig. 1). Such cavities are now realizable with the development of ultrahigh reflectivity, low-loss dielectric layered mirrors, with a total loss coefficient (including scattering and absorption) $\mathcal{L}=1.6\times10^{-6}$ [12]. High-Q cavities have been used to observe cavity QED effects at optical frequencies in the strong coupling regime [13], such as optical bistability [14] and vacuum Rabi splitting [15]. We modify

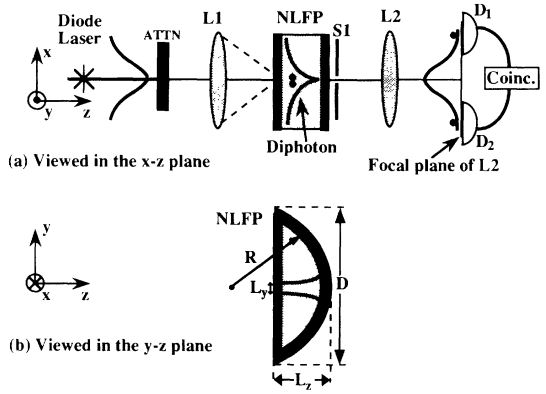

FIG. 1. Schematic of the nonlinear Fabry-Pérot resonator (NLFP) used to observe the diphoton [(a) viewed in the x-z plane and (b) in the y-z plane (not drawn to scale)]. The NLFP consists of one planar mirror and one cylindrical mirror with radius of curvature R and diameter D, filled with Cs vapor. The Gaussian mode is sketched in (b). Radiation from a diode laser is tuned above the $D2$ resonance, attenuated, and coupled into the NLFP by cylindrical lens L1. The diphoton is a resonance in the two-photon transmission function, with relative-coordinate wave function shown in (a). Slit S1 filters the unbound component, and the remaining photons are detected in coincidence as a function of the spacing of detectors D_1 and D_2. The resulting Lorentzian-squared two-point correlation function is sketched in (a).

this system by (1) exciting the atomic vapor off resonance so that it acts as a passive Kerr medium, self-focusing when excited above, and self-defocusing when excited below resonance, and by (2) using cylindrical mirrors with wavelength-scale spacing, rather than spherical mirrors, to obtain a 1D quantum field. As an aside, we note that a Fabry-Pérot cavity with planar mirrors operating in the fundamental longitudinal mode is the optical equivalent of a quantum well, providing a means to study the dynamics of the interacting 2D Bose gas. The equivalence of these nonlinear optical field theories to theories for interacting bosons in condensed matter systems in one or two dimensions provides intriguing possibilities for optical experiments to test predictions made for a dilute Bose gas [16]. In contrast to experiments conducted in superfluid ^{4}He films, the photonic system allows experimental control over the interaction coupling strength and does not require the use of low temperature techniques.

We study the experimental feasibility of detecting the diphoton by the following approach. We first consider solutions inside a perfectly reflecting hemicylindrical cavity (i.e., there is one planar mirror and one cylindrical mirror; see Fig. 1), and treat the Cs vapor as a lossless self-focusing Kerr medium. Because the cavity mode spacing is much larger than the bandwidth of the highly resonant $\chi^{(3)}$ nonlinearity, there is negligible photon-photon scattering into initially unoccupied modes. The quantum theory for the slowly varying envelope of the excited mode is equivalent to that for a nonrelativistic gas of massive bosons, with an effective mass on the order of $\hbar\omega/c^2$, and pairwise attractive delta-function interactions between the photons, arising from the exchange of virtual atomic excitations [2]. When imperfect reflectivity and absorption in the vapor are taken into account, the diphoton is interpreted as a two-photon Fabry-Pérot transmission resonance, which is broadened by the cavity linewidth.

The classical dynamics for the slowly varying electric field envelope for one polarization is obtained from the ansatz

$$E(x,t)=\mathrm{Re}\{\mathcal{E}(x,t)\phi(y,z)\exp(-i\omega_0 t)\}\,. \tag{1}$$

Here

$$\phi(y,z)=\left(\frac{L_y}{w(z)}\right)^{1/2}\exp\left\{-\frac{y^2}{w(z)^2}\right\}\sin\left(\frac{ky^2}{2R(z)}+\frac{l\pi z}{L_z}\right) \tag{2}$$

is a cylindrical Gaussian mode, with $w(z)$ and $R(z)$ the usual local beam radius and wave-front radius of curvature, respectively [17]. A narrow bandwidth envelope allows the material to respond adiabatically, so the propagation equation in the paraxial (slowly varying envelope) approximation is the NLSE,

$$\frac{i}{v_g}\frac{\partial\mathcal{E}}{\partial t}=-\frac{1}{2k_0}\frac{\partial^2\mathcal{E}}{\partial x^2}-\Gamma\frac{\omega_0}{c}n_2|\mathcal{E}|^2\mathcal{E}\,, \tag{3}$$

where the nonlinear index coefficient is $n_2=3\pi\chi^{(3)}/2n_0$, and Γ is a mode overlap factor [9]. For operation near the fundamental mode $L_z\ll k_0L_y^2$ and $\Gamma\approx 3\sqrt{8}$.

To quantize the field we rescale the envelope relative to the vacuum fluctuation amplitude inside the cavity,

$$\mathcal{E}(x,t)=4(2\pi)^{1/4}\left(\frac{\hbar\omega_0}{L_yL_z}\right)^{1/2}\psi(x,t)\,, \tag{4}$$

so that, to lowest order in the paraxial approximation, the energy in the empty cavity is

$$\begin{aligned}U&=\int_{\text{cavity}}\frac{E^2+B^2}{8\pi}d^3x\\&=\hbar\omega_0\int|\psi|^2dx+\frac{\hbar v_g}{2k_0}\int\left|\frac{\partial\psi}{\partial x}\right|^2dx\,.\end{aligned} \tag{5}$$

In this approximation, the quantum field theory is formally equivalent to a nonrelativistic many-body theory for the complex scalar field ψ, which satisfies the standard Bose equal-time commutation relations, $[\psi(x,t),\psi^\dagger(x',t)]=\delta(x-x')$ [18]. The energy Eq. (5) is the free-field Hamiltonian, with the first term playing the role of the rest mass energy, and the second the kinetic energy, with effective mass $m=\hbar v_g/k_0\approx\hbar\omega_0/c^2$. We follow the dynamics of the envelope field ψ in the "envelope picture" [19] in which the operators evolve according to the carrier wave Hamiltonian [the "rest mass"

term in Eq. (5), which cancels the rapid oscillation of the carrier wave $\exp(-i\omega_0 t)$ in Eq. (1)], and the states evolve by the remaining slow terms. The interaction Hamiltonian is chosen so that the Heisenberg equations of motion reduce to the NLSE in the classical limit. The normally ordered envelope Hamiltonian satisfying these conditions is

$$H_{\rm env}=\frac{\hbar^2}{2m}\int dx\frac{\partial\psi^\dagger}{\partial x}\frac{\partial\psi}{\partial x}-\frac{G}{2}\int dx_1dx_2\psi^\dagger(x_1)\psi^\dagger(x_2)\delta(x_1-x_2)\psi(x_1)\psi(x_2)\,, \tag{6a}$$

where the coupling constant

$$G=12\sqrt{\pi}\frac{v_g}{c}\frac{(\hbar\omega_0)^2n_2}{L_yL_z} \tag{6b}$$

varies directly with n_2 and inversely with the confinement area L_yL_z. Solving for the stationary states of $H_{\rm env}$ in the two-body sector is equivalent, after separating out the free center-of-mass motion, to a 1D Schrödinger equation for a reduced particle with an attractive delta-function potential at the origin. The sole bound state has the wave function

$$u(x_1-x_2)=\sqrt{2d}\exp\left\{-\frac{|x_1-x_2|}{2d}\right\}, \tag{7a}$$

$$d=\frac{\hbar^2}{mG}=\frac{1}{48\pi^{3/2}}\frac{\lambda^2L_yL_z}{n_2\hbar\omega_0}\,, \tag{7b}$$

where $v_g\approx c/n_0\approx c$, for an alkali vapor detuned sufficiently from resonance. The binding energy is

$$E_d=\frac{mG^2}{4\hbar^2}=\hbar\omega_0\Delta n_d\,, \tag{8a}$$

$$(\Delta n)_d=n_2\frac{3\sqrt{\pi}\hbar\omega_0}{dL_yL_z}\,, \tag{8b}$$

where we have identified the binding energy with the effective nonlinear index shift of the diphoton Δn_d, Eq. (8b).

Production and detection of these quasiparticles depends crucially on the material response. Cs vapor is an excellent candidate for the nonlinear medium due to the large oscillator strength of the $D2$ line, and high vapor pressure at room temperature. When tuning close to resonance to achieve large nonlinearities, absorption in the vapor dominates the Q of the cavity. The reduction of Q leads to a larger cavity linewidth which poses two possible problems: (1) The diphoton resonance may overlap with the continuum of unbound states; (2) the diphoton width may be larger than the detuning (which dominates the width of the material response), thus invalidating the adiabatic response susceptibility model. Problem (1) may be overcome by additional spatial filtering of the output, but problem (2) determines the optimal range of detunings by requiring that the linear absorptivity α be small (cavity linewidth narrow) while the nonlinear index n_2 is still large. Figure 2 shows plots of n_2 and α for the $D2$ line of Cs. The relative locations of the "knees" of these curves show that one can obtain large nonlinearities with small absorption by detuning above resonance near the knee of the Doppler-broadened n_2 curve. The model used to generate these curves includes the hyperfine structure of Cs; it will be presented elsewhere. A typical operating point is $\Delta\nu=1.9\times\Delta\nu_D=780$ MHz (above resonance), which yields $n_2=7.5\times10^{-5}$ esu $=6.3\times10^{-7}$ cm^2/W, and $\alpha=6.5\times10^{-2}$ cm^{-1}.

Finally, we consider the design of the cavity. For ease of alignment, we propose to use a hemicylindrical cavity. Tight focusing in the y direction and closely spaced mirrors will ensure maximum confinement of the fields. In Fig. 1 the dimension D, the spacing L_z, and the radius of curvature R are related by $D=2(2L_zR)^{1/2}$ for $L_z\ll R$. For $D=1$ mm and $L_z=3\lambda/2$, $R=1.2\times10^5\lambda=10$ cm, and the transverse mode spot size is $L_y=12\lambda=10$ μm. The longitudinal and transverse mode spacings are, respectively, $\delta\nu_z=c/2L_z=1.2\times10^{14}$ Hz and $\delta\nu_y=c\lambda/4\pi^2L_y^2=7\times10^{10}$ Hz; both spacings are much larger than the bandwidth of the resonant nonlinearity. With the mirrors used by Rempe *et al.* [12], the cavity quality factor is $Q=\omega_0/c(\alpha+\mathcal{L}/L_z)=10^6$, with a linewidth $\delta\nu_{\rm cav}=\nu_0/Q=370$ MHz. Since this linewidth is smaller than the detuning, the suceptibility model is acceptable.

For these parameters the diphoton has a spatial width $d=62$ μm, and binding energy $E_d/h=430$ MHz. Because of the finite lifetime $\tau=Q/\omega_0=0.4$ ns, the two-photon eigenstates have a linewidth on the order of

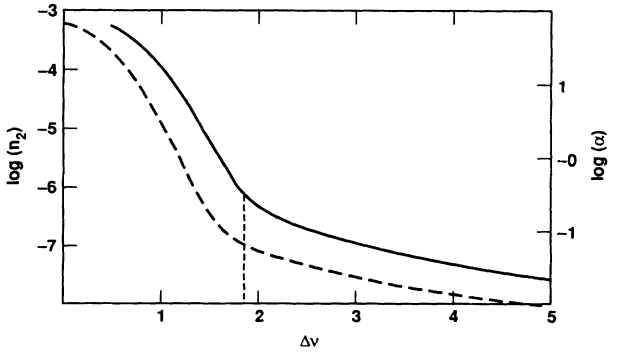

FIG. 2. Plots of the nonlinear index coefficient n_2 (solid curve with values on the left-hand axis in cm^2/W) and linear absorption coefficient α (dashed curve with values on the right-hand axis in cm^{-1}) vs the detuning (above the $6P_{3/2}F=5$ excited state) in units of the Doppler width $\Delta\nu_D$, for Cs vapor at $T=350$ K, $N=2.7\times10^{12}$ cm^{-3}, when pumping out of the $6S_{1/2}F=4$ ground state. Contributions from all other allowed $6P_{3/2}$ hyperfine levels, including interference effects, have been included. The vertical dashed line represents the operating point $\Delta\nu=1.9\Delta\nu_D$ used in the text.

$\delta\nu_{cav}=370$ MHz. A schematic diphoton detection experiment is depicted in Fig. 1. Coherent radiation from a tunable source, such as a diode laser, is incident on the quantum wire. By attenuating the power so that, on average, there is less than one photon in the cavity at a given time, the probability of occupation of the mode by more than two photons is rendered negligible. Coincidence counting of the photons measures the steady-state two-photon spatial correlation function. For this purpose, the quantum wire can be viewed as a filter for the two-photon eigenstates of H_{env} [Eq. (6a)], passing those states which satisfy the energy conservation condition,

$$\left|2\hbar\omega_{injected}-\left(2\hbar\omega_0+\frac{\hbar K^2}{4m}+E_{rel}\right)\right|\lesssim O(\hbar\delta\nu_{cav})\,, \qquad (9)$$

where $\hbar K$ is the center-of-mass momentum and E_{rel} is the energy of the relative motion. When the injected signal is tuned below the empty-cavity resonance frequency by half the bound-state energy (i.e., $\omega_{inj}=\omega_0-E_d/2\hbar$), then in the limit of zero cavity linewidth it follows from Eq. (9) that the quantum wire will reject all states except diphotons with $K=0$. Rejection of the unbound components can still be achieved for small but nonzero cavity linewidth, because of the energy gap between the diphoton and the continuum. However, when the cavity linewidth is on the order of the diphoton "ionization" energy, as in the system we have analyzed, there is substantial overlap between the diphoton resonance and the continuum. The resulting spurious counts can be reduced by additional spatial filtering. Note that when two photons make successive round trips in the cavity, the diphoton component maintains its spatial profile, whereas the unbound component diffuses from the initial focal spot. In an unfolded cavity picture, this is equivalent to the familiar statement that the transverse profile of the diphoton is unchanged by propagation, while the unbound component diffracts. To estimate this effect, we calculate the time for the variance $(\Delta x)^2$ of the unbound component to spread, as a free wave packet, to twice an initial value of $\Delta x=d$; the result is $t_{spread}=2\sqrt{2}\pi d^2/c\lambda=0.13$ ns. Thus, within the cavity lifetime (0.4 ns) the unbound component spreads and becomes small over relative distances on the order of the diphoton width; therefore it can be filtered from the coincidence counts by an exit aperture slightly larger than d. The photons are detected in coincidence in the far field of lens L2, which Fourier transforms the correlation function. If the detector resolution is shorter than the cavity lifetime (i.e., resolution better than 0.4 ns, which has been demonstrated [20]), the far-field spatial correlation function will be a squared Lorentzian [the absolute square of the Fourier transform of $u(x_1-x_2)$, Eq. (7a)] which falls off algebraically as the fourth power of the relative distance between detectors D_1 and D_2. This is the characteristic signature of the diphoton.

We thank E. M. Wright and H. L. Morrison for stimulating discussions. I.H.D. and R.Y.C. acknowledge support by ONR under Grant No. N00014-90-J-1259, and J.C.G. by the U.S. Department of Energy at the Lawrence Livermore National Laboratory under Contract No. W-7405-Eng-48.

[1] H. Haug and S. W. Koch, *Quantum Theory of the Optical and Electronic Properties of Semiconductors* (World Scientific, New Jersey, 1990).
[2] R. Y. Chiao, I. H. Deutsch, and J. C. Garrison, Phys. Rev. Lett. **67**, 1399 (1991).
[3] R. Y. Chiao, E. Garmire, and C. H. Townes, Phys. Rev. Lett. **13**, 479 (1964).
[4] A. Barthelemy, S. Maneuf, and C. Froehly, Opt. Commun. **55**, 201 (1985).
[5] J. S. Aitchinson *et al.*, Opt. Lett. **15**, 471 (1990).
[6] G. R. Allan *et al.*, Opt. Lett. **16**, 157 (1991).
[7] C. R. Nohl, Ann. Phys. (N.Y.) **96**, 234 (1976).
[8] Y. Lai and H. A. Haus, Phys. Rev. A **40**, 844 (1989); **40**, 1138 (1989).
[9] E. M. Wright, Phys. Rev. A **43**, 3836 (1991).
[10] P. D. Drummond and S. J. Carter, J. Opt. Soc. Am. B **4**, 1565 (1987); P. D. Drummond, S. J. Carter, and R. M. Shelby, Opt. Lett. **14**, 373 (1989); P. D. Drummond and S. J. Carter, Phys. Rev. A **42**, 2966 (1990); M. Rosenbluth and R. M. Shelby, Phys. Rev. A **34**, 3974 (1986).
[11] B. Yurke and M. J. Potasek, J. Opt. Soc. Am. B **6**, 1227 (1989).
[12] G. Rempe *et al.*, Opt. Lett. **17**, 363 (1991).
[13] E. A. Hinds, Adv. At. Mol. Opt. Phys. **28**, 237 (1991).
[14] G. Rempe *et al.*, Phys. Rev. Lett. **67**, 1727 (1991).
[15] R. J. Thompson *et al.*, Phys. Rev. Lett. **68**, 1132 (1992).
[16] R. Y. Chiao, I. H. Deutsch, J. C. Garrison, and E. M. Wright, in "Serge Ahkmanov: A Memorial Volume," edited by H. Walther (Adam-Hilger, Bristol, to be published).
[17] A. Yariv, *Quantum Electronics* (Wiley, New York, 1989), 3rd ed., p. 118.
[18] I. H. Deutsch and J. C. Garrison, Phys. Rev. A **43**, 2498 (1991).
[19] I. H. Deutsch and J. C. Garrison, Opt. Commun. **86**, 311 (1991).
[20] S. Cova, A. Longoni, and G. Ripamonti, IEEE Trans. Nucl. Sci. **29**, 599 (1982).

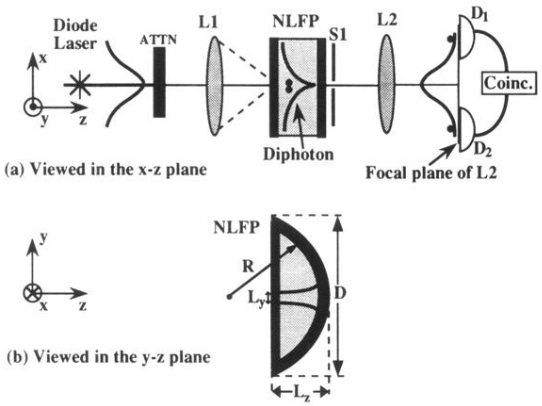

FIG. 1. Schematic of the nonlinear Fabry-Pérot resonator (NLFP) used to observe the diphoton [(a) viewed in the x-z plane and (b) in the y-z plane (not drawn to scale)]. The NLFP consists of one planar mirror and one cylindrical mirror with radius of curvature R and diameter D, filled with Cs vapor. The Gaussian mode is sketched in (b). Radiation from a diode laser is tuned above the $D2$ resonance, attenuated, and coupled into the NLFP by cylindrical lens L1. The diphoton is a resonance in the two-photon transmission function, with relative-coordinate wave function shown in (a). Slit S1 filters the unbound component, and the remaining photons are detected in coincidence as a function of the spacing of detectors D_1 and D_2. The resulting Lorentzian-squared two-point correlation function is sketched in (a).